Acta Cryst. (1981). B37, 495–499

FeB–CrB Stacking Variants in the System GdNi–TbNi

BY K. KLEPP AND E. PARTHÉ

Laboratoire de Cristallographie aux Rayons X, Université de Genève, 24 quai Ernest Ansermet, CH-1211 Genève 4, Switzerland

(*Received* 29 *July* 1980; *accepted* 8 *September* 1980)

Abstract

In the system $Gd_{1-x}Tb_xNi$ three mixed FeB–CrB stacking variants have been found, all having monoclinic symmetry with space group $P2_1/m$. $Gd_{0.4}Tb_{0.6}Ni$ with base-structure stacking $h_2c_3h_2c_2$: $a = 32{\cdot}49\ (7)$, $b = 4{\cdot}226\ (6)$, $c = 5{\cdot}478\ (8)$ Å, $\beta = 101{\cdot}9\ (2)°$, $Z = 18$, $R = 0{\cdot}091$; $Gd_{0.3}Tb_{0.7}Ni$ with base-structure stacking h_2c_2: $a = 14{\cdot}35\ (2)$, $b = 4{\cdot}201\ (2)$, $c = 5{\cdot}458\ (4)$ Å, $\beta = 100{\cdot}6\ (1)°$, $Z = 8$; $Gd_{0.2}Tb_{0.8}Ni$ with base-structure stacking h_2c: $a = 10{\cdot}67\ (2)$, $b = 4{\cdot}195\ (4)$, $c = 5{\cdot}457\ (8)$ Å, $\beta = 97{\cdot}2\ (2)°$, $Z = 6$, $R = 0{\cdot}071$. The refined lattice constants of TbNi, low-temperature modification, are $a = 21{\cdot}34\ (4)$, $b = 4{\cdot}197\ (2)$, $c = 5{\cdot}458\ (3)$ Å, $\beta = 97{\cdot}1\ (1)°$. A study of the possible space groups of FeB–CrB stacking variants indicates that six space groups can occur depending on the symmetry of the Zhdanov stacking symbol.

Introduction

It has recently been shown that FeB–CrB stacking variants are formed in $R_{1-x}R'_xNi$ systems where R = Gd and R' = Dy, Y (Klepp & Parthé, 1980). In the course of a more detailed study of these stacking variants it was of interest to investigate the pseudobinary system GdNi–TbNi for their formation. TbNi itself crystallizes with an FeB–CrB stacking variant (Lemaire & Paccard, 1970), with 66·7% hexagonal base-structure stacking (low-temperature modification), while GdNi adopts the CrB structure type (0% hexagonal base-structure stacking).

Sample preparation

Samples in the system $Gd_{1-x}Tb_xNi$ were prepared from metals of high purity (Gd, Tb 99·9%, Ni 99·99%) by conventional arc-melting techniques. The ingots thus obtained were wrapped in Ta foil and sealed in evacuated silica tubes. They were annealed at 1073 K for five weeks and then allowed to cool slowly in the furnace.

Derivation of stacking variant from unit-cell data

Powder diagrams taken with a Guinier–de Wolff camera (Cu $K\alpha$ radiation) indicated the existence of three ternary phases $Gd_{0.4}Tb_{0.6}Ni$, $Gd_{0.3}Tb_{0.7}Ni$ and $Gd_{0.2}Tb_{0.8}Ni$. The diffraction diagrams of the latter two showed close similarities to those of the FeB–CrB stacking variants $Gd_{0.55}Dy_{0.45}Ni$ and $Gd_{0.7}Y_{0.3}Ni$ reported previously (Klepp & Parthé, 1980), whereas the powder pattern of $Gd_{0.4}Tb_{0.6}Ni$ was of a new type.

Small single crystals of irregular shape were isolated from all three alloys. Crystallographic investigations showed that they had monoclinic symmetry with systematic extinctions for $0k0$: $k = 2n + 1$, indicating $P2_1/m$ or $P2_1$ as possible space groups. Precise lattice constants were determined on a four-circle diffractometer (Philips PW 1100) with graphite-monochromated Mo $K\alpha$ radiation ($\lambda = 0{\cdot}71069$ Å). Translation periods of a number of reciprocal-lattice rows were measured from which the lattice constants were refined by *PARAM* (XRAY system, 1976). The cell dimensions for these three compounds are listed in Table 1 together with those of TbNi which have been redetermined by the same method.

$Gd_{0.2}Tb_{0.8}Ni$

The unit-cell data indicated a similarity with $Gd_{0.7}Y_{0.3}Ni$, which has h_2c base-structure stacking.

Table 1. *Crystallographic data for* FeB–CrB *stacking variants in the quasibinary section* $Gd_{1-x}Tb_xNi$ (*annealed at* 1073 K)

Composition	$Gd_{0.4}Tb_{0.6}Ni$	$Gd_{0.3}Tb_{0.7}Ni$	$Gd_{0.2}Tb_{0.8}Ni$	TbNi(l.t.)*
Base-structure stacking	$h_2c_3h_2c_2$	h_2c_2	h_2c	h_4c_2
Percentage of hexagonal base-structure stacking	44·4%	50%	66·7%	66·7%
Space group	$P2_1/m$	$P2_1/m$	$P2_1/m$	$P2_1/m$
Z	18	8	6	12
a (Å)	32·49 (7)	14·35 (2)	10·67 (2)	21·34 (4)
b (Å)	4·226 (6)	4·201 (2)	4·195 (4)	4·197 (2)
c (Å)	5·478 (8)	5·458 (4)	5·457 (8)	5·458 (3)
β (°)	101·9 (2)	100·6 (1)	97·2 (2)	97·1 (1)

* For data of TbNi (low-temperature modification) according to Lemaire & Paccard (1970) see text.

0567-7408/81/030495-05$01.00

However, since the stackings h_2c and h_4c_2 cannot be distinguished unambiguously from powder diagrams, it was decided to study and refine the structure of $Gd_{0.2}Tb_{0.8}Ni$ by single-crystal methods. To avoid any pitfalls with the cell determined by the peak-hunting program (which indicated h_2c), the cell chosen for the data collection was purposely doubled along a (in order to correspond to h_4c_2). However, no reflection belonging to this larger cell alone was above the background level.

$Gd_{0.3}Tb_{0.7}Ni$

A comparison between observed and calculated powder intensities obtained with *LAZY PULVERIX* (Yvon, Jeitschko & Parthé, 1977) allowed us to ascertain that this compound has a structure isotypic with $Gd_{0.55}Dy_{0.45}Ni$ with base-structure stacking h_2c_2.

$Gd_{0.4}Tb_{0.6}Ni$

On the basis of the lattice dimensions of $Gd_{0.4}Tb_{0.6}Ni$ it could be concluded that this compound was also an FeB–CrB stacking variant. The problem of structure determination was therefore mainly to find out the correct stacking sequence, which was accomplished from the unit-cell relationships for FeB–CrB stacking variants derived previously (Klepp & Parthé, 1980). By application of equation (17*a*) in Klepp & Parthé (1980), the number of stacking steps in the sequence, $p + n$,* was determined to be 9. The number of uncompensated sideways displacements, $p - n$,* can be derived from equation (18). In the present case, however, considering the error limits of the measured unit cell, this equation gave two acceptable solutions, one with $p - n = 1$ and the other with $p - n = 5$. According to Klepp & Parthé (1981), for $p + n = 9$ there are altogether 21 stacking possibilities, 14 of which have space group $P2_1/m$ (see below). Considering only the stacking variants for $p - n = 1$ and $p - n = 5$, this number reduces to 10. On the other hand it could be assumed from previously obtained experimental results on $Gd_{1-x}R_xNi$ alloys (R = Dy, Y) that also in the $Gd_{1-x}Tb_xNi$ system the percentage of hexagonal base-structure stacking increases with x. Thus, the percentage of hexagonal stacking for $Gd_{0.4}Tb_{0.6}Ni$ had to have a value between 0% (c stacking for GdNi) and 50% (h_2c_2 stacking for $Gd_{0.3}Tb_{0.7}Ni$). With this limitation, the number of possible stackings reduced to three for $p - n = 1$ and to four for $p - n = 5$. For the remaining seven stacking possibilities, powder diffraction diagrams were calculated with *LAZY PULVERIX* (Yvon, Jeitschko & Parthé, 1977). Comparison with the observed diffraction diagram indicated that the stacking sequence is $h_2c_3h_2c_2$. This result was corroborated by the single-crystal structure refinement.

* v and h in equations (16*a*), (16*d*), (17*a*), (17*b*), (18) and (21) of Klepp & Parthé (1980) should be substituted by $p + n$ and $p - n$ respectively in order to achieve consistency with the terminology used by Patterson & Kasper (1967) to describe close packing.

Structure refinement

Intensities were collected for $Gd_{0.4}Tb_{0.6}Ni$ and $Gd_{0.2}Tb_{0.8}Ni$ with Mo $K\alpha$ radiation (θ–2θ scan mode, $6 \leq 2\theta \leq 54°$). Two sets of symmetry-independent reflections were measured for each crystal. Background, Lorentz and polarization corrections were applied and absorption effects were accounted for by a spherical absorption correction ($\mu R = 2{\cdot}6$ for $Gd_{0.4}Tb_{0.6}Ni$, $\mu R = 2{\cdot}0$ for $Gd_{0.2}Tb_{0.8}Ni$). Equivalent reflections were averaged yielding unique sets of 669 and 244 observed reflections, respectively.

The structures of $Gd_{0.4}Tb_{0.6}Ni$ and $Gd_{0.2}Tb_{0.8}Ni$ were refined by full-matrix least squares with *CRYLSQ* of the XRAY system (1976). A random distribution of the two rare-earth atoms was assumed and their

Table 2. *Positional and thermal parameters of* $Gd_{0.4}Tb_{0.6}Ni$ *and* $Gd_{0.2}Tb_{0.8}Ni$

The space group is $P2_1/m$. All atoms are on equipoint 2(*e*). Random distribution of the rare-earth atoms is assumed, the occupation ratio of the rare-earth atoms in the individual sites being identical with the ratio given by the overall chemical formula. The isotropic temperature factor is expressed as $T = \exp(-2\pi^2 Us^2)$, where $s = 1/d_{hkl}$, U is in $Å^2 \times 10^4$. (The values for the isotropic temperature factors are obtained by recalculation from the anisotropic ones. E.s.d.'s are given in parentheses.)

	x	y	z	U
$Gd_{0.4}Tb_{0.6}Ni$				
$R(1)$	0·0401 (1)	0·25	0·1820 (7)	130 (10)
$R(2)$	0·1513 (1)	0·25	0·0763 (7)	140 (10)
$R(3)$	0·2618 (1)	0·25	0·4409 (7)	160 (10)
$R(4)$	0·3734 (1)	0·25	0·3380 (7)	130 (10)
$R(5)$	0·4844 (1)	0·25	0·2337 (7)	131 (9)
$R(6)$	0·5955 (1)	0·25	0·1302 (7)	130 (10)
$R(7)$	0·7067 (1)	0·25	0·0235 (7)	170 (10)
$R(8)$	0·8176 (1)	0·25	0·3897 (7)	150 (10)
$R(9)$	0·9288 (1)	0·25	0·2875 (7)	130 (10)
Ni(1)	0·0082 (3)	0·25	0·636 (2)	160 (30)
Ni(2)	0·1197 (3)	0·25	0·529 (2)	180 (30)
Ni(3)	0·2298 (3)	0·25	0·908 (2)	170 (30)
Ni(4)	0·3413 (3)	0·25	0·792 (2)	160 (30)
Ni(5)	0·4523 (3)	0·25	0·688 (2)	170 (30)
Ni(6)	0·5634 (3)	0·25	0·583 (2)	160 (30)
Ni(7)	0·6747 (3)	0·25	0·476 (2)	140 (30)
Ni(8)	0·7859 (3)	0·25	0·858 (2)	210 (30)
Ni(9)	0·8973 (3)	0·25	0·744 (2)	170 (30)
$Gd_{0.2}Tb_{0.8}Ni$				
$R(1)$	0·1198 (6)	0·25	0·8948 (9)	140 (40)
$R(2)$	0·4539 (7)	0·25	0·742 (1)	130 (30)
$R(3)$	0·7869 (6)	0·25	0·5833 (9)	120 (40)
Ni(1)	0·025 (2)	0·25	0·380 (3)	190 (90)
Ni(2)	0·357 (2)	0·25	0·211 (3)	220 (90)
Ni(3)	0·690 (2)	0·25	0·053 (3)	200 (100)

positional and thermal parameters were restricted to have identical values. Scattering factors for neutral atoms (Cromer & Mann, 1968) were used and anomalous-dispersion corrections (*International Tables for X-ray Crystallography*, 1974) applied. Refinement with isotropic temperature factors converged to $R = 0{\cdot}10$ ($Gd_{0.4}Tb_{0.6}Ni$) and $R = 0{\cdot}091$ ($Gd_{0.2}Tb_{0.8}Ni$). Introduction of anisotropic thermal parameters led to the final R of 0·091 [$R_w = 0{\cdot}092$, $w = 1/\sigma^2(F)$, 1144 contributing reflections: 669 + 475 weak reflections which calculate greater than the observed] for $Gd_{0.4}Tb_{0.6}Ni$ and $R = 0{\cdot}071$ [$R_w = 0{\cdot}096$, $w = 1/\sigma^2(F)$, 244 contributing reflections] for $Gd_{0.2}Tb_{0.8}Ni$. The structural data of both compounds are listed in Table 2.*

Results

A drawing of the $Gd_{0.4}Tb_{0.6}Ni$ structure is shown in Fig. 1. Drawings for the two other structures which are isotypic with $Gd_{0.55}Dy_{0.45}Ni$ ($Gd_{0.3}Tb_{0.7}Ni$) and $Gd_{0.7}Y_{0.3}Ni$ ($Gd_{0.2}Tb_{0.8}Ni$) can be found in the previous publication (Klepp & Parthé, 1980).

The interatomic distances for $Gd_{0.4}Tb_{0.6}Ni$ and $Gd_{0.2}Tb_{0.8}Ni$ are listed in Tables 3 and 4 respectively. As can be seen from the R–R distances, both

* Lists of structure factors and anisotropic thermal parameters for $Gd_{0.4}Tb_{0.6}Ni$ and $Gd_{0.2}Tb_{0.8}Ni$ have been deposited with the British Library Lending Division as Supplementary Publication No. SUP 35716 (17 pp.). Copies may be obtained through The Executive Secretary, International Union of Crystallography, 5 Abbey Square, Chester CH1 2HU, England.

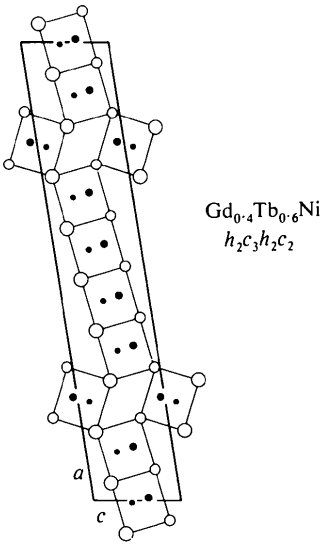

$Gd_{0.4}Tb_{0.6}Ni$
$h_2c_3h_2c_2$

Fig. 1. Projection of the unit cell of $Gd_{0.4}Tb_{0.6}Ni$ along [010]. Open circles correspond to rare-earth atom sites, full circles represent the sites of the Ni atoms. Small circles are at height $\frac{1}{4}$, large circles at height $\frac{3}{4}$. The drawing displays idealized point positions derived from periodic unit-cell twinning.

Table 3. *Interatomic distances* (Å) *in* $Gd_{0.4}Tb_{0.6}Ni$ *up to* 4 Å

E.s.d.'s are in parentheses, $R \equiv Gd_{0.4}Tb_{0.6}$.

Ni(1)–	R(9)	2·873 (13)	Ni(2)–	R(1)	2·874 (13)
	R(1)	2·886 (13)		R(2)	2·875 (13)
	2R(9)	2·910 (8)		2R(8)	2·905 (8)
	2R(1)	2·927 (9)		2R(9)	2·936 (9)
	R(1)	2·955 (12)		R(2)	2·961 (12)
	2Ni(1)	2·578 (9)		2Ni(9)	2·580 (8)
	Ni(9)	3·768 (17)		Ni(3)	3·745 (17)
	Ni(2)	3·787 (17)		Ni(1)	3·787 (17)
Ni(3)–	R(2)	2·886 (13)	Ni(4)–	R(3)	2·884 (13)
	R(3)	2·890 (12)		R(4)	2·892 (13)
	2R(8)	2·907 (8)		2R(6)	2·914 (8)
	2R(7)	2·923 (8)		2R(7)	2·928 (9)
	R(3)	2·955 (15)		R(4)	2·954 (12)
	2Ni(8)	2·577 (10)		2Ni(7)	2·566 (8)
	Ni(2)	3·745 (17)		Ni(5)	3·764 (17)
	Ni(4)	3·806 (17)		Ni(3)	3·806 (17)
Ni(5)–	R(4)	2·864 (13)	Ni(6)–	R(5)	2·867 (13)
	R(5)	2·893 (13)		R(6)	2·885 (13)
	2R(5)	2·917 (8)		2R(4)	2·914 (8)
	2R(6)	2·917 (9)		2R(5)	2·922 (9)
	R(5)	2·954 (12)		R(6)	2·961 (13)
	2Ni(6)	2·574 (9)		2Ni(5)	2·574 (9)
	Ni(4)	3·764 (17)		Ni(5)	3·773 (17)
	Ni(6)	3·773 (17)		Ni(7)	3·780 (16)
Ni(7)–	R(7)	2·882 (13)	Ni(8)–	R(8)	2·883 (13)
	2R(3)	2·921 (8)		R(7)	2·899 (13)
	2R(4)	2·934 (9)		2R(2)	2·909 (8)
	R(4)	2·934 (9)		2R(3)	2·914 (9)
	R(7)	2·962 (12)		R(8)	2·956 (14)
	2Ni(4)	2·566 (8)		2Ni(3)	2·577 (10)
	Ni(8)	3·779 (17)		Ni(7)	3·779 (17)
	Ni(6)	3·780 (16)		Ni(9)	3·801 (17)
Ni(9)–	R(9)	2·890 (13)	R(1)–2R(9)		3·566 (7)
	R(8)	2·895 (13)		2R(1)	3·615 (9)
	2R(1)	2·902 (8)		2R(9)	3·630 (7)
	2R(2)	2·930 (9)		R(2)	3·776 (10)
	R(9)	2·943 (12)		R(9)	3·777 (10)
	2Ni(2)	2·580 (8)			
	Ni(1)	3·768 (17)			
	Ni(8)	3·801 (17)			
R(2)–2R(8)		3·580 (7)	R(3)–2R(7)		3·588 (7)
	2R(9)	3·614 (9)		2R(8)	3·603 (7)
	2R(8)	3·616 (7)		2R(7)	3·614 (8)
	R(3)	3·730 (12)		R(2)	3·730 (12)
	R(1)	3·776 (10)		R(4)	3·783 (10)
R(4)–2R(6)		3·571 (7)	R(5)–2R(5)		3·575 (7)
	2R(7)	3·610 (9)		2R(6)	3·611 (9)
	2R(6)	3·624 (7)		2R(5)	3·622 (7)
	R(5)	3·766 (10)		R(4)	3·766 (10)
	R(3)	3·783 (10)		R(6)	3·769 (10)
R(6)–2R(4)		3·571 (7)	R(6)–2R(3)		3·588 (7)
	2R(5)	3·611 (9)		2R(4)	3·610 (9)
	2R(4)	3·624 (7)		2R(3)	3·614 (7)
	R(5)	3·769 (10)		R(8)	3·743 (12)
	R(7)	3·777 (10)		R(6)	3·777 (10)
R(8)–2R(2)		3·580 (7)	R(9)–2R(1)		3·566 (7)
	2R(3)	3·603 (7)		2R(2)	3·614 (9)
	2R(2)	3·616 (7)		2R(1)	3·630 (7)
	R(7)	3·743 (12)		R(8)	3·770 (10)
	R(9)	3·770 (10)		R(1)	3·777 (10)

compounds obey closely the geometrical requirement for ideal stacking derived previously: each R has six nearly equidistant R neighbours.

$Gd_{0.4}Tb_{0.6}Ni$ is the sixth mixed FeB–CrB stacking variant found in rare-earth–nickel systems. Mixed FeB–CrB stacking variants were recently reported by Fornasini & Merlo (1980) for ThNi with base-structure stacking $(hc)_2$ and interestingly also for α-CaCu with base-structure stacking $(hchch)_2$, β-CaCu with base-structure stacking hc_2hc and SrAg with base-structure stacking $(hc)_2$ (Merlo & Fornasini, 1981). However, the number of mixed FeB–CrB stacking variants is still too small to derive any systematics concerning the formation of a particular stacking sequence.

It is in this respect interesting that a comparatively small substitution of Tb by Gd leads to a change of the stacking sequence (h_4c_2 to h_2c) which is not accompanied by a change in the percentage of hexagonal stacking.

The redetermined and refined unit-cell data of TbNi allow an unambiguous choice of unit cell to be made which agrees with equation (16). This cell is distinguishable from other possible cells because the projection of its a axis, $a\sin(\beta - 90)$, is equal to the displacement caused by the uncompensated stacking steps:

$$(p-n)\frac{a_{FeB}}{2}\tan\psi.$$

With the unit-cell setting chosen by Lemaire & Paccard (1970) our refined values give $a = 21{\cdot}36$ (4), $b = 4{\cdot}197$ (2), $c = 5{\cdot}458$ (3) Å, $\beta = 97{\cdot}6$ (1)° instead of $a = 21{\cdot}26$ (3), $b = 4{\cdot}21$ (1), $c = 5{\cdot}45$ (1) Å, $\beta = 97{\cdot}4$ (3)°. Application of equation (18) leads to an h (or $p - n$) value of 2·18 indicating that this is not the cell which corresponds to our convention. Transformation to the unit cell listed in Table 1 results in $p - n = 2{\cdot}03$, which is a value close enough to an integer to leave no doubt that this is the unit cell to choose.

Table 4. *Interatomic distances* (Å) *in* $Gd_{0.2}Tb_{0.8}Ni$ *up to* 4 Å

E.s.d.'s are in parentheses, $R \equiv Gd_{0.2}Tb_{0.8}$

Ni(1)–	$R(1)$	2·862 (15)	Ni(2)–	$R(1)$	2·877 (18)
	$R(3)$	2·893 (19)		$R(2)$	2·880 (17)
	$2R(3)$	2·894 (13)		$2R(2)$	2·902 (13)
	$2R(1)$	2·907 (11)		$2R(3)$	2·904 (13)
	$R(1)$	2·954 (17)		$R(2)$	2·953 (16)
	2Ni(1)	2·560 (12)		2Ni(3)	2·557 (11)
	Ni(2)	3·770 (26)		Ni(3)	3·767 (26)
	Ni(3)	3·787 (24)		Ni(1)	3·770 (26)
Ni(3)–	$R(2)$	2·856 (18)	$R(1)$–$2R(3)$		3·577 (7)
	$R(3)$	2·879 (17)		$2R(3)$	3·584 (8)
	$2R(1)$	2·906 (13)		$2R(1)$	3·604 (9)
	$2R(2)$	2·907 (13)		$R(3)$	3·740 (12)
	$R(3)$	2·950 (15)		$R(2)$	3·761 (12)
	2Ni(2)	2·557 (11)			
	Ni(2)	3·767 (26)			
	Ni(1)	3·787 (24)			
$R(2)$–$2R(2)$		3·548 (8)	$R(3)$–$2R(1)$		3·577 (7)
	$2R(2)$	3·606 (9)		$2R(1)$	3·584 (8)
	$2R(3)$	3·607 (9)		$2R(2)$	3·607 (9)
	$R(1)$	3·761 (12)		$R(1)$	3·740 (12)
	$R(3)$	3·762 (12)		$R(2)$	3·762 (12)

Possible space groups for FeB–CrB stacking variants

Once the unit cell is known, further information about the space group can considerably limit the number of stacking variants to be considered in a model calculation. For the derivation of the space groups of FeB–CrB stacking variants, it is advantageous to disregard for the moment the Ni atoms and consider only the stacking of the rectangular buckled layers of rare-earth atoms (Fig. 2). The symmetry elements within one layer are two mutually perpendicular mirror planes ($\perp$ to b_{FeB} and $\perp$ to c_{FeB}) and a diagonal glide plane in the layer ($\perp$ to the two mirror planes). If the layers were stacked directly one above the other, this would result in space group *Pmmn*. The stacking operations actually occurring, however, lead to a displacement in the direction of c_{FeB}. From a given layer, two stacking positions (+ and −) are available and the stacking system may therefore be referred to as doubly connected (Beck, 1967). This allows one to apply the Jagodzinski–Wyckoff as well as the corresponding Zhdanov notation for the description of these sequences. It is characteristic of the FeB–CrB stacking system that the sideways displacement of a stacking step is not a simple rational fraction of the translation period in the corresponding direction. It is therefore in general not possible in the course of stacking to arrive at a layer with an identical position to the starting layer unless the numbers of positive and negative stacking steps are equal ($p = n$). The symmetry of any arrangement of stacked buckled rare-earth layers and also of the Ni-centred FeB–CrB stacking variants is uniquely determined by the symmetry of a single-stacked layer and the symmetry properties of the stacking sequence. The symmetry properties of stacking sequences have been studied by Patterson & Kasper (1967), who introduced Zhdanov

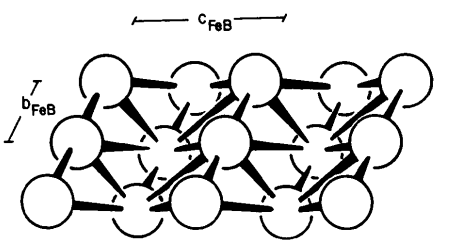

Fig. 2. Perspective view of the buckled rare-earth layer, which is found in all FeB–CrB stacking variants.

Table 5. *Survey of possible space groups for* FeB–CrB *stacking variants*

The space groups are given in the standard setting. Reference to equivalent axes of the FeB cell is made in the footnote. The symmetry of the stacking sequence corresponding to a given space group is, where possible, denoted by special symbols (see text) which are written below the space-group symbol.

$p+n$	Orthorhombic $p-n=0$	Monoclinic $p-n\geq 0$	Orthorhombic $p-n=1$
1			*Cmcm**
Even, ≥2	*Pnma*† | – () – | – () – |		
Any, ≥3		$P2_1/m$† – () – () –	
Even, ≥6	$Pmn2_1$‡ | – | – |		
Any, ≥7		*Pm*†	
Even, ≥12	$Pmc2_1$§		

* $c \triangleq b_{FeB}$.
† $b \triangleq b_{FeB}$, $c \triangleq c_{FeB}$.
‡ $a \triangleq b_{FeB}$, $b \triangleq c_{FeB}$.
§ $a \triangleq b_{FeB}$, $c \triangleq c_{FeB}$.

formulae which were complemented by special symmetry symbols. According to the symmetry properties of the stacking sequence, six different space groups are possible for FeB–CrB stacking variants. Each of these space groups will have a mirror plane originating from the mirror plane of the individual layer ($\perp$ to b_{FeB}) which is not affected by the stacking.

(*a*) An asymmetric stacking sequence, such as $4\underline{3}\underline{1}1$, leads to space group *Pm*.

(*b*) A symmetrical stacking sequence where the numbers of like sign in the Zhdanov symbols are mirrored, such as $(4)\underline{3}1(\underline{2})1\underline{3}$, leads to an inversion centre and a twofold screw axis. The corresponding space group is $P2_1/m$.

(*c*) An antisymmetrical stacking sequence where the numbers of opposite sign are mirrored in the Zhdanov symbol, such as $|2\underline{1}1|\underline{1}\underline{2}|$, retains the diagonal glide plane of the layers. The space group is $Pmn2_1$.

(*d*) A stacking sequence consisting of two subperiods with opposite signs, such as $3\underline{2}1\underline{3}2\underline{1}$, leads to a glide plane, the corresponding space group being $Pmc2_1$.

(*e*) A stacking sequence meeting the conditions (*b*), (*c*) and (*d*), such as $|1(\underline{2})1|\underline{1}(2)\underline{1}|$, leads to space group *Pnma*.

(*f*) In the special case that $p + n = 1$, the space group is *Cmcm* as found with the CrB type.

The different possibilities, together with the corresponding minimum values of $p + n$ (see Table 1, Klepp & Parthé, 1981), are listed in Table 5.

This study was supported by the Swiss National Science Foundation under contract No. 2.601-0.80.

References

BECK, P. A. (1967). *Z. Kristallogr.* **124**, 101–114.

CROMER, D. T. & MANN, J. B. (1968). *Acta Cryst.* A**24**, 321–324.

FORNASINI, M. L. & MERLO, F. (1980). Joint Italo-Swiss Meeting on Crystallography, Crystal Growth and Materials Science, Trento, Collected Abstracts pp. 54–57.

International Tables for X-ray Crystallography (1974). Vol. IV. Birmingham: Kynoch Press.

KLEPP, K. & PARTHÉ, E. (1980). *Acta Cryst.* B**36**, 774–782.

KLEPP, K. & PARTHÉ, E. (1981). *Acta Cryst.* A**37**, 61–65.

LEMAIRE, R. & PACCARD, D. (1970). *J. Less-Common Met.* **21**, 403–413.

MERLO, F. & FORNASINI, M. L. (1981). *Acta Cryst.* B**37**, 500–503.

PATTERSON, A. L. & KASPER, J. S. (1967). *International Tables for X-ray Crystallography*, Vol. II. Birmingham: Kynoch Press.

XRAY system (1976). Tech. Rep. TR-446. Computer Science Center, Univ. of Maryland, College Park, Maryland.

YVON, K., JEITSCHKO, W. & PARTHÉ, E. (1977). *J. Appl. Cryst.* **10**, 73–74.